THE JOURNAL OF PHYSICAL CHEMISTRY B

Article

Cite This: J. Phys. Chem. B 2018, 122, 6471−6482

pubs.acs.org/JPCB

Effects of Urea and TMAO on Lipid Self-Assembly under Osmotic Stress Conditions

Quoc Dat Pham,*[,†] Amanuel Wolde-Kidan,[‡] Anirudh Gupta,[‡] Alexander Schlaich,[‡] Emanuel Schneck,[§] Roland R. Netz,[‡] and Emma Sparr[†]

[†]Division of Physical Chemistry, Chemistry Department, Lund University, P.O. Box 124, 22100 Lund, Sweden

[‡]Fachbereich Physik, Freie Universität Berlin, Arnimallee 14, 14195 Berlin, Germany

[§]Department of Biomaterials, Max Planck Institute of Colloids and Interfaces, Am Mühlenberg 1, 14476 Potsdam, Germany

Supporting Information

ABSTRACT: Most land-living organisms regularly experience dehydration. In nature, one commonly applied strategy to protect against this osmotic stress is to introduce small polar molecules with low vapor pressure, commonly called osmolytes. Two examples of naturally occurring small polar compounds are urea and trimethylamine *N*-oxide (TMAO), which are known to have counteracting effects on protein stability. In this work, we investigate the effects of urea and TMAO on lipid self-assembly at varying water contents, focusing on dehydrated conditions. By using complementary experimental techniques, including sorption microcalorimetry, NMR, and X-ray scattering, together with molecular dynamics simulations in model systems composed of phosphatidylcholine lipids, water, and solute, we characterize interactions and self-assembly over a large range of hydration conditions. It is shown that urea and TMAO show qualitatively similar effects on lipid self-assembly at high water contents, whereas they have clearly different effects in dehydrated conditions. The latter can be explained by differences in the molecular interactions between the solutes and the lipid headgroups. TMAO is repelled from the bilayer interface, and it is thereby expelled from lipid lamellar systems with low water contents and narrow inter-bilayer regions. In these conditions, TMAO shows no effect on the lipid phase behavior. Urea, on the other hand, shows a slight affinity for the lipid headgroup layer, and it is present in the lipid lamellar system at all water contents. As a result, urea may exchange with water in dry conditions and thereby prevent dehydration-induced phase transitions. In nature, urea and TMAO are sometimes found together in the same organisms and it is possible that their combined effect is to both protect lipid membranes against dehydration and still avoid denaturation of proteins.

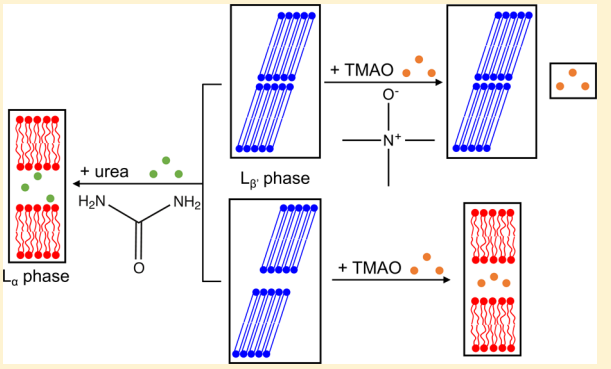

INTRODUCTION

Most organisms in nature are in one way or another affected by osmotic stress of water. Plants and seeds can be exposed to dry and cold climate and soil with high salinity, marine life is exposed to high salinity in ocean water, and many organisms and higher animals have to deal with desiccating conditions in the form of low relative humidity (RH) and cold climate. These situations may cause an imbalance between the internal and external osmotic pressure. Such osmotic stress can lead to changes in macromolecular self-assembled structures. In lipid membranes, dehydration due to osmotic stress may lead to phase transitions, lateral segregation, and membrane fusion, which in turn influence membrane barrier functions.[1,2] For example, dehydration-induced phase transitions between different lipid self-assembled structures have been associated with dehydration-induced cell injury in plant leaves[3] and altered barrier function of the human skin.[4−7] In protein systems, osmotic stress can influence protein conformations and folding.[8,9]

In nature, one generally applied strategy for protection against osmotic stress is to introduce small polar molecules with low vapor pressure, generally referred to as osmolytes or compatible solutes.[10−12] Plants exposed to regular night frosts can produce fructan for protection,[13] and some primitive animals use trehalose to survive the winter,[14] whereas seaweed and marine algae can regulate the osmotic pressure of the saline water through production of, e.g., glycerol.[15] Many insects experience evaporative water loss, and some freeze-tolerant insects show pronounced glycerol synthesis.[16] Also, in higher animals, polar cosolutes are considered to protect the cell membranes against osmotic stress. Deep-sea elasmobranchs

Received: March 4, 2018
Revised: April 25, 2018
Published: April 25, 2018

DOI: 10.1021/acs.jpcb.8b02159
J. Phys. Chem. B 2018, 122, 6471−6482

(sharks, skates, and rays) living under conditions of high salinity, high pressure, and low temperature have high concentrations of urea and trimethylamine-*N*-oxide (TMAO) (up to 600 mM).[17,18] The human skin contains a mixture of small polar compounds that is referred to as the "natural moisturizing factor" (NMF), comprising free amino acids, amino acid derivatives, lactic acid, urea, and glycerol.[19−21] The manifestation of NMF components in the stratum corneum (SC) is well characterized, and their presence is considered crucial to maintain SC softness and pliability in dehydrated conditions.[21,22] Defective skin conditions and certain skin diseases, for example, winter xerosis and atopic dermatitis, are associated with decreased NMF levels in the SC.[23,24] Small polar solutes are also utilized in many technical applications. For example, sugars or glycerol are often added to dry lipid-based formulations to prevent phase segregation or precipitation[25] and some of these compounds are also used as "moisturizers" in skin care products.[26] For long-term storage of proteins, osmolytes, like glycerol, are commonly added to the solution before freezing to stabilize proteins.

The examples listed above all illustrate how relatively simple small polar solutes can act to protect macromolecular complex systems against osmotic stress. The molecular mechanisms behind this protection will vary between the different solutes, solution conditions, and macromolecules. Osmolyte molecules are often classified on the basis of their effects on protein assembly, as they may either stabilize or denature folded proteins. A large class of naturally occurring stabilizing osmolytes combine a molecular dipole moment with hydrophobicity in the form of methyl groups located around the positively charged part of the molecule. TMAO is one example of such dipolar/hydrophobic osmolytes. Denaturing molecules, like urea, do not have the same proportion of hydrophobicity and dipolarity.[27] It is interesting to note that there are several examples where these two classes of molecules have been found to coexist in the same organisms[10,11,17,18] and their counteracting effect on proteins is rather well characterized in excess solution conditions.[11,28−30] The same osmolytes may also influence the lipid self-assembly in biological membranes. Previous studies on urea, glycerol, and sugars have shown that small polar molecules with low vapor pressure can act by replacing water in the drying system, thereby protecting self-assembled structures that are otherwise only present in hydrated conditions.[31−33] A similar mechanism where polar solutes replace water in lipid self-assembled systems has also been put forward for glycerol and sugars in excess solution conditions,[34,35] whereas other solutes, like TMAO, cause an increased attraction between phospholipid bilayers in excess solution by being expelled from the lamellar phase.[36]

In the present study, we investigate the effects of two different polar solutes, urea and TMAO, on lipid lamellar systems in osmotic stress conditions. These polar solutes were chosen due to their similarities in terms of size and because of their opposite effects on protein stability. Focus is laid on how these polar solutes influence lipid self-assembly and phase transitions in conditions of low water contents. The model systems are composed of either dimyristoylphosphatidylcholine (DMPC) or palmitoyl-oleoyl-phosphatidylcholine (POPC). The DMPC model systems were chosen to enable studies of hydration-induced phase transitions between lamellar gel phase ($L_{\beta'}$)[a] bilayers with ordered and rigid chains or liquid crystalline (L_α) bilayers with fluid/disordered chains.[1] The POPC model systems allow for studies of gradual hydration of fluid bilayers over a large range of water contents.[37] We use complementary experimental techniques, including sorption microcalorimetry, NMR, as well as small- and wide-angle X-ray scattering (SAXS and WAXS), together with molecular dynamics (MD) simulations, to characterize the hydration of phospholipid bilayers in the presence of the solutes at varying relative humidities and constant temperature (T = 27 °C).

MATERIALS AND METHODS

Sample Preparation. DMPC and POPC were purchased from Avanti Polar Lipids, Inc. (Alabaster, AL). Urea and TMAO were obtained from Sigma-Aldrich. The samples were prepared so that the mass fraction of urea or TMAO in the dry samples, $\Phi^{\text{lipid}}_{\text{solute}} = m_{\text{solute}}/(m_{\text{solute}} + m_{\text{lipid}})$, was fixed and the water content may vary. Experiments were performed for samples with compositions of $\Phi^{\text{lipid}}_{\text{solute}}$ 0−10 wt %. The samples were mixed together by the use of a mortar and pestle to produce a fine powder mixture and then submitted for further drying under vacuum with a 3 Å molecular sieve for at least one day. According to Nilsson et al.[38] and Mcintosh et al.,[39] such a careful drying procedure is sufficient to remove all water from the lipid sample. The dry samples were then loaded into the calorimetry cell in a glovebox under a stream of dry N_2. Samples for NMR and scattering measurements were equilibrated at 27 °C in closed chambers for 3−4 days with a relative humidity (RH) of 43, 84, and 96%, controlled with saturated solutions of K_2CO_3, KCl, and K_2SO_4, respectively.

Sorption Microcalorimetry. A double twin isothermal microcalorimeter was used to study the thermodynamics of the water vapor sorption.[40,41] The instrument involves a two-chamber calorimetric cell, with a sorption chamber that contains the dry sample and a vaporization chamber in which liquid water is injected to start the sorption experiment. The chambers are connected by a tube. Water vaporizes in the vaporization chamber and diffuses through the tube to the sorption chamber where it is absorbed by the sample. The calorimetric cell is inserted into a double twin isothermal microcalorimeter that separately measures thermal powers released/absorbed in the two chambers. From this method, one can simultaneously monitor the relative humidity, the partial molar enthalpy of mixing of water (sorption enthalpy, $\Delta H_{\text{sorp}} = \partial H/\partial n_{\text{w}}$), and the water uptake.[40] The experimental setup can be considered a continuous titration of an initially dry sample with water vapor. The data for each experiment were recorded for ca. 14 days at 27 °C.

Solid-State NMR. Site-specific qualitative information about molecular mobility can be obtained by comparing signal intensities acquired with cross-polarization (CP),[42] insensitive nuclei enhanced by polarization transfer (INEPT),[43] and direct polarization (DP) set of experiments in polarization transfer solid-state NMR (PT ssNMR), where DP is used as a reference. The CP[42] and INEPT[43] schemes for $^1H \rightarrow {}^{13}C$ polarization transfer are commonly used to enhance the ^{13}C signal in NMR. NMR experiments were performed at ^1H and ^{13}C resonance frequencies of 500 and 125 MHz, respectively, on a Bruker Avance AVII—500 NMR spectrometer equipped with a Bruker Efree 4 mm magic-angle spinning (MAS) probe. Prior to measurement, all samples which had been pre-equilibrated at controlled RH were equilibrated in the NMR spectrometer for at least an hour at 27 °C, which had been calibrated at 5 kHz MAS using the ^1H chemical shift of methanol.[44] The following setup was used: spectral width of 248.5 ppm, acquisition time of 0.05 s, 64 scans per experiment, recycle delay of 5 s, and ^1H

DOI: 10.1021/acs.jpcb.8b02159
J. Phys. Chem. B 2018, 122, 6471−6482

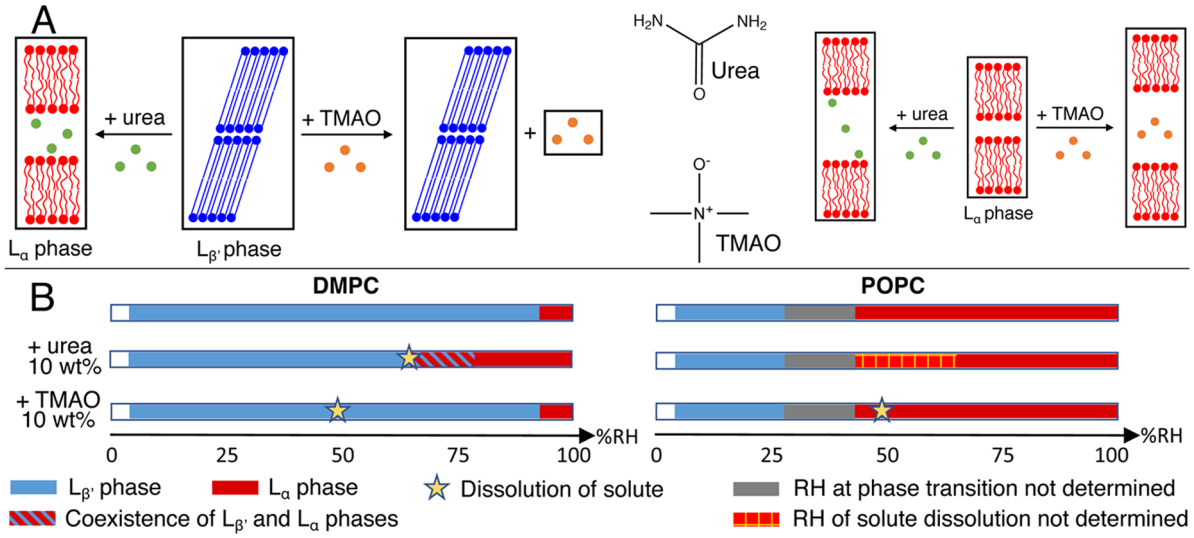

Figure 1. Schematic summary of the effects of urea and TMAO on phase behavior and hydration of phospholipid bilayers. (A) Illustration of the effect of urea and TMAO on lipid lamellar phase behavior with ordered and rigid chains in dehydrated conditions, here denoted $L_{\beta'}$ (left), and a bilayer with fluid acyl chains, L_α, in hydrated conditions (right). Chemical structures of urea and TMAO are also shown. (B) Summary of lipid phase behavior at varying RH in the presence and absence of solutes urea and TMAO.

and ^{13}C hard pulses at $\omega_1^{H/C}/2\pi$ = 80.6 kHz. All experiments were carried out at a spinning frequency of 5 kHz and recorded under 68 kHz two-pulse phase modulation ^1H.[45] The ^1H nutation frequency was ramped up from 72 to 88 kHz during the contact time of 1 ms in the CP experiment. The INEPT experiments were performed with the delay times τ of 1.8 ms and τ' of 1.2 ms. The data were processed with a line broadening of 20 Hz, zero-filling from 1024 to 8192 time-domain points, Fourier transform, and phase and baseline correction by inhouse Matlab code partially from matNMR.[46] The chemical shift of the INEPT methyl peak at 14.2 ppm was used as an internal reference, whereas for the samples without INEPT signal, the calibration from previous experiments was kept.

The basis of the PT ssNMR experiment is to compare the signal intensities acquired from three different experiments (DP, CP,[42] and INEPT)[43] comprised in a set of PT ssNMR and performed on the same sample, yielding information about the rate and anisotropy of the C−H bond reorientation, as quantified by the correlation time τ_c and order parameter $|S_{CH}|$.[47] The DP spectrum generally shows resonances from all carbons in the sample and acts as a reference. CP is efficient in boosting the signal of segments with reorientation slower than τ_c = 10 ns and/or more anisotropic than $|S_{CH}|$ = 0.02. The signal from mobile segments with motion faster than τ_c = 0.1 μs and anisotropy lower than $|S_{CH}|$ = 0.2 is selectively enhanced in INEPT spectra.

SAXS and WAXS. SAXS and WAXS were performed to determine the lamellar periodicity and the packing order of the lipid chains, respectively. The experiments were carried out using a SAXLab's GANESHA 300 XL SAXS system (JJ X-ray, Denmark) equipped with a microfocus sealed tube X-ray source (GE's Inspection Technology) and a PILATUS solid-state two-dimensional photon counting detector (Dectris, Switzerland). Different q ranges were accessed by adjusting the distance between the sample and detector. The scattering vector q is defined as $q = (4\pi \sin\theta)/\lambda$, where θ is half of the scattering angle and λ = 1.54 Å is the X-ray wavelength. All samples were measured in a specially designed "sandwich cell", where the sample which had been pre-equilibrated at controlled RH is contained between two mica sheets. The samples were equilibrated at 27 °C in a temperature-controlled sample holder in the instrument for at least 5 h before measurement.

MD Simulations. Single periodically replicated hydrated planar DMPC and POPC bilayers were simulated. Pre-equilibrated membrane systems in the liquid state L_α were used as the starting structure.[48] For the simulations, the GROMACS 2016.3 software package was used. The simulation box with dimensions d_x, d_y, and d_z contained one lipid bilayer composed of n_{lipid} = 72 DMPC or POPC molecules (36 in each monolayer) hydrated with a fixed number of water molecules n_{water}. The level of hydration is defined as the number of water molecules per lipid n_{water}/n_{lipid}. The amount of solutes (TMAO or urea) added is 1 and 10 wt % of the corresponding lipid bilayer to match the experimental concentrations. The membranes are arranged parallel to the (x,y)-plane without any position restraints and stabilized by the hydrophobic effect. Periodic boundary conditions in all spatial directions are used. In this way, a periodic stack of infinitely extended phospholipid membranes that interact across thin layers of water (with or without added solute) is atomistically represented. In our simulations, we used the Berger lipid force field for the lipid membranes,[49] together with the SPC/E water model.[50] Thermodynamically optimized force fields were used for TMAO[27] and urea.[51] The simulations were performed in the NpT ensemble at atmospheric pressure (1 bar), with a time step of Δt = 2 fs. Temperature was controlled using the velocity-rescale thermostat,[52] with a time constant of τ_t = 0.5 ps. The pressure was controlled semi-isotropically using the Berendsen barostat,[53] with a time constant of τ_p = 2 ps and a compressibility of $\kappa = 4.5 \times 10^{-5}$ bar^{-1}. We used a Lennard-Jones cutoff of 0.9 nm with a potential shift and accounted for the electrostatic interactions using the particle-mesh-Ewald method with a 0.9 nm real space cutoff. All simulations were performed at T = 27 °C and equilibrated for 50 ns before a production run of again 50 ns.

DOI: 10.1021/acs.jpcb.8b02159
J. Phys. Chem. B 2018, 122, 6471−6482

RESULTS AND DISCUSSION

We here investigate the effects of urea and TMAO on lipid self-assembly under osmotic stress conditions. An overview of the main findings is shown in Figure 1. It is shown that urea and TMAO have clearly different effects on lipid self-assembly in dry conditions. Urea stabilizes fluid lamellar structures in dehydrated conditions, whereas TMAO has no effect on the lipid phase behavior at low water contents. In hydrated systems, on the other hand, urea and TMAO have very similar effects on the self-assembly, both leading to increased swelling of the lamellar liquid crystalline phase. Below, we separately discuss the experimental findings for urea and TMAO in the different phospholipid systems. This is followed by a description of the simulation results. The results are then collected into a unified description of the phase behavior to support the conclusions illustrated in Figure 1.

Sorption Microcalorimetry Characterization of Phospholipid Hydration and Solute Dissolution. The calorimetric sorption measurement provides a relation between the water content and the water chemical potential ($\Delta\mu_w$), expressed in terms of the RH as

$$\Delta\mu_w = -RT \ln(\mathrm{RH}/100) \quad (1)$$

where RH is given in percent, R is the gas constant, and T is the temperature. These data are presented as sorption isotherms, presenting water uptake as a function of RH. $\Delta\mu_w$ can also be expressed in terms of osmotic pressure (Π_{osm}) as $\Delta\mu_w = -V_w\Pi_{osm}$, where V_w is the molar volume of pure water (Figures 2A and S1). In simultaneous measurements, the partial molar enthalpy of water (called sorption enthalpy) is obtained, $\Delta H_{sorp} = \partial H/\partial n_w$, for the whole range of water contents.

To enable the interpretation of the data obtained for the ternary lipid–solute–water systems, we first present reference data for the binary lipid–water and solute–water systems. The sorption microcalorimetry data for the binary systems of DMPC–water and POPC–water are shown in Figure 2. For DMPC, the uptake of the first 1–2 water molecules gives rise to an exothermic peak (Figure 2B, blue curve), which is interpreted as being due to the water molecules that interact strongly with the oxygen atoms of the choline phosphate groups.[40,54] This hydration step also leads to the formation of the $L_{\beta'}$ lamellar gel phase.[1] The simultaneously measured sorption isotherm of DMPC (Figure 2A, blue curve) shows a gradual but small uptake of water over a large span in relative humidities up to 93% RH. This reflects the swelling of the $L_{\beta'}$ phase. Further increase in the relative humidity leads to a transition between $L_{\beta'}$ and L_α phases.[1,40] This is observed as a stepwise increase in water content at constant RH = 93% in the sorption isotherm (Figure 2A). The transition can also be identified in the enthalpy curve for DMPC (Figure 2B, blue curve) as a region with positive and constant ΔH_{sorp}. The endothermic nature of this process is consistent with the interpretation that the main molecular event is the melting of the alkyl chains.[40] At even higher water contents, the whole sample forms the L_α phase and ΔH_{sorp} drops to a small but positive value, which then gradually decreases toward zero when approaching saturation humidity (Figure 2B). In the sorption isotherm, this corresponds to the regime with continuous increase of the water content toward the swelling limit. In the regime where there is a swelling of the L_α phase, the enthalpy and the free energy have opposite signs and it is therefore concluded that the swelling of the lamellar L_α phase toward full hydration is entropy driven.[40]

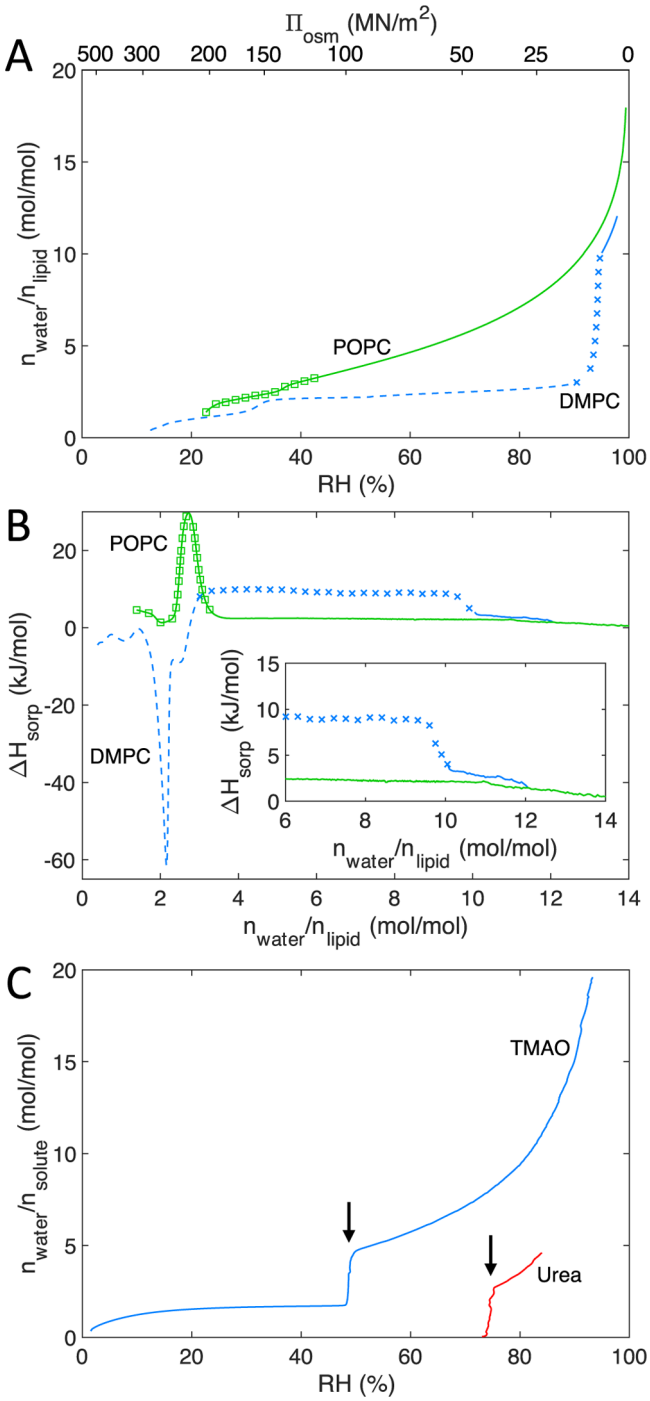

Figure 2. (A, B) Microcalorimetric sorption data for DMPC and POPC at 27 °C. (A) Sorption isotherm giving water content (n_{water}/n_{lipid}) versus relative humidity (% RH) (bottom axis) and the corresponding osmotic pressure of water (Π_{osm}) (top axis). (B) Sorption enthalpy of water, ΔH_{sorp}, as a function of water content. The phase behavior is represented by: $L_{\beta'}$ gel phase (- -), fluid L_α phase (—), and coexistence of $L_{\beta'}$ and L_α phases (xxx). For the POPC system, the exact position of the L_α–$L_{\beta'}$ phase transition was not determined and it occurs within the RH regime denoted (□□□). Inset in (B) shows a magnification of the ΔH_{sorp} at high water content. (C) Sorption isotherm of neat urea and TMAO. The arrows indicate the dissolution of the solid compounds.

DOI: 10.1021/acs.jpcb.8b02159
J. Phys. Chem. B 2018, 122, 6471–6482

The binary POPC–water system differs from the binary DMPC–water system in that the POPC L_α phase is stable at much lower relative humidities. The sorption isotherm of POPC shows a gradual uptake of water over a large relative humidity range, with a tiny vertical step at $n_{water}/n_{lipid} \approx 3$ at 37% RH (Figure 2A, green curve). In separate SAXS and WAXS experiments, it was confirmed that POPC forms a lamellar phase with rigid chains in the completely dry sample, whereas at 43% RH (corresponding to $n_{water}/n_{lipid} \approx 4$), only the L_α phase is present (Figure S2).[37] The observed endothermic signal (i.e., $\Delta H_{sorp} > 0$) at low water contents ($n_{water}/n_{lipid} \approx 2–3$, Figure 2B, green curve) can be interpreted as the combined heat effects from melting of the alkyl chains and primary hydration of the headgroups. At higher relative humidities, there is a continuous swelling of the POPC L_α phase, which is associated with small but positive ΔH_{sorp}. It is also noticed that the sorption isotherms for the POPC and DMPC L_α phases are very similar for high relative humidities (Figure 2A, RH > 93%).

Experiments were also performed for the binary systems of solute (urea or TMAO) and water (Figures 2C and S3A,B). The vapor pressure over a saturated solution of urea in water is 74% RH at 27 °C. Solid powder of urea does not absorb any detectable amount of water at RH < 74%, whereas there is a sharp increase in water uptake at RH = 74% to the saturation concentration ($n_{water}/n_{urea} = 3$) (Figure 2C, red curve), which is associated with an endothermic ΔH_{sorp} (Figure S3A). The dissolution step is followed by a continuous uptake of water when the relative humidity increases, which is associated with the dilution of the aqueous urea solution. The sorption isotherm of TMAO (Figure 2C, blue curve) shows uptake of water already in the dry sample, leading to the formation of TMAO dihydrate,[55] which is associated with a strong exothermic enthalpy change (Figure S3B). At 49% RH, the solid TMAO dihydrate is dissolved to its saturation concentration. This is detected as a step corresponding to $n_{water}/n_{TMAO} \approx 3$ in the sorption isotherm at RH 49%, associated with an endothermic enthalpy change. Finally, the dissolution step is followed by a continuous dilution of the aqueous TMAO solution with increasing relative humidity. The enthalpy of dilution of both solutes is positive and decays toward zero with increasing relative humidity (Figure S3A,B).

Urea Stabilizes Fluid Lamellar Structures in Dehydrated Conditions. The addition of urea has strong influence on both hydration-induced phase changes and swelling in phospholipid systems. The hydration process was followed in sorption microcalorimetry experiments (Figures 3 and S3C), and phase characterization was done for selected RH conditions using SAXS and WAXS (Figure S2, Table S1) and PT ssNMR (Figure 4). The inset panels in Figure 3A,C show the experimental isotherms for the ternary systems with compositions $\Phi_{urea}^{lipid} = 10$ wt %, together with the isotherm calculated as a linear combination of the isotherms for binary lipid–water and urea–water systems with the appropriate proportions. As the calculated and experimental data do not overlap, we conclude that the hydration process in the ternary systems is not simply the sum of the processes in the binary systems, implying that there are additional interactions to be considered. One striking observation is that the dissolution of urea is strongly altered when present in the lipid systems. This is apparent from the shifts of the dissolution step in the isotherms (indicated with arrows in Figure 3A, Table S2), which is also consistent with previous studies.[32] The dissolution of urea

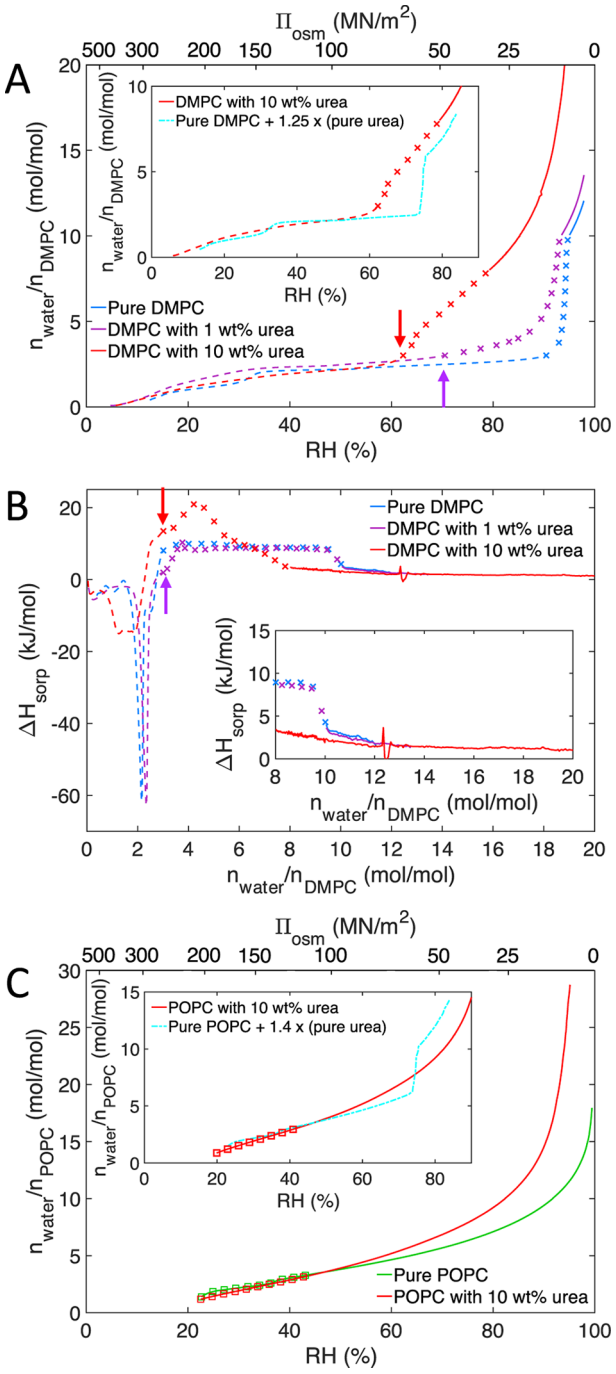

Figure 3. Microcalorimetric sorption data for DMPC and urea (A, B), $\Phi_{urea}^{DMPC} = 0$, 1, and 10 wt % (blue, purple, and red curves, respectively) and POPC and urea (C), $\Phi_{urea}^{POPC} = 0$ and 10 wt % (green and red curves, respectively). (A, C) Sorption isotherms giving water content (n_{water}/n_{lipid}) versus relative humidity (% RH) (bottom axis) and the corresponding osmotic pressure of water (Π_{osm}) (top axis). (B) Sorption enthalpy of water, ΔH_{sorp}, as a function of water content. The arrows indicate the dissolution of the urea. The phase behavior is represented as follows: $L_{\beta'}$ gel phase (- -), fluid L_α phase (—), coexistence of $L_{\beta'}$ and L_α phases (xxx), and the region where $L_{\beta'}$–L_α transition occurs (exact position not determined) (□□□). Inset in (B) shows a magnification of the ΔH_{sorp} at high water content. Insets in (A, C): comparison between the experimental sorption isotherms for samples with composition $\Phi_{urea}^{lipid} = 10$ wt % (red line), and a theoretical isotherm (cyan line) calculated as the linear combination of the experimental isotherms for the binary systems of lipid–water and urea–water with the right proportion to match $\Phi_{urea}^{lipid} = 10$ wt %.

DOI: 10.1021/acs.jpcb.8b02159
J. Phys. Chem. B 2018, 122, 6471–6482

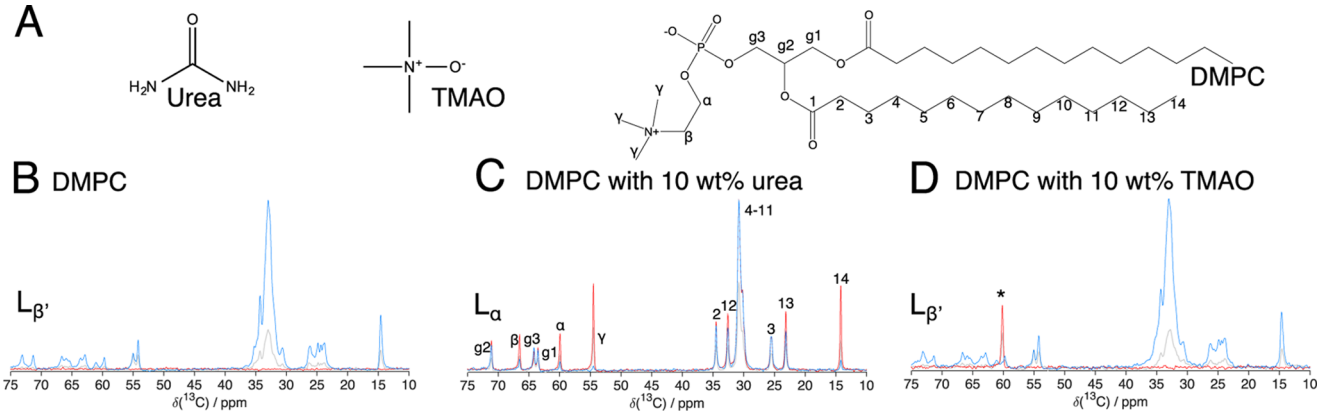

Figure 4. (A) Chemical structures of urea, TMAO, and DMPC with numbered segments. (B–D) ^{13}C MAS NMR spectra (DP: gray, CP: blue, INEPT: red) of DMPC (B) and DMPC with 10 wt % urea (C) or TMAO (D) at RH 84% and 27 °C. The absence of INEPT signal in pure DMPC (B) and DMPC with TMAO (D) signifies the rigid phase. The coexistence of INEPT and CP signals with the same line shape in the spectra of DMPC with urea (C) indicates an anisotropic liquid crystalline phase reorienting with $\tau_c < 0.1$ μs and $0.02 < |S_{CH}| < 0.2$. The resonance of TMAO marked with asterisk is only observed in the INEPT spectrum, implying that the motion of this solute is fast and isotropic.

cannot be resolved in the POPC–urea–water isotherms, which might be explained by the fact that the dissolution of urea occurs gradually over a range of relative humidities when present in the fluid lamellar phase.

To illustrate the effects on lipid phase behavior, we will first discuss in detail the system of DMPC with relatively high content of urea, Φ_{urea}^{DMPC} = 10 wt %. For this system, urea dissolves at RH = 62%. At lower relative humidities, urea is present as a solid powder together with the DMPC lamellar gel $L_{\beta'}$ phase. As solid urea does not take up water, the isotherms for the ternary systems in Figure 3A are completely dominated by the sorption behavior of the DMPC $L_{\beta'}$ phase for this RH interval. At RH = 62%, urea is dissolved in the DMPC lamellar system, thereby affecting both the swelling of the lamellar phases and the overall phase behavior (Figure 3A,B). In particular, the addition of urea alters the position of the $L_{\beta'}$–L_α phase transition toward lower relative humidities. The assignments of the coexistence regions (Figure 3 and Table S1) were based on the combined sorption and enthalpy data together with PT ssNMR experiments for selected RH values (Figure 4). For the Φ_{urea}^{DMPC} = 10 wt % sample, the $L_{\beta'}$–L_α transition coincides with the dissolution of urea and the enthalpy curve shows an endothermic regime at n_{water}/n_{lipid} = 3–8 (Figure 3B) that is associated with both these events. The PT ssNMR experiments confirm a rigid lipid phase for the DMPC system (Figure 4A) and an anisotropic liquid crystalline phase for DMPC with 10 wt % urea (Figure 4B) at RH 84%. Similar trends were also found at lower urea contents. At the lowest urea concentration investigated (Φ_{urea}^{DMPC} = 1 wt %), urea is dissolved at RH 72% in the $L_{\beta'}$ phase, and the $L_{\beta'}$–L_α phase transition takes place at 87–93% RH (Figure 3A).

For both the DMPC and POPC systems, a single L_α phase forms at high RH values. A comparison between the sorption curves (Figure 3A,C) shows that the samples that contain urea also contain more water compared to the binary lipid–water system at the same relative humidity. The hydration of the L_α phase is associated with small and positive ΔH_{sorp}. The enthalpy has the opposite sign relative to the free energy, thus again demonstrating that the swelling process is entropy driven. We finally note that the effects of urea in the L_α phase are quantitatively very similar for the DMPC and POPC L_α phases at high relative humidities (Figure S4).

TMAO is Expelled from the Dehydrated Solid Lamellar Phases. In clear contrast to urea, TMAO shows no detectable effects on lipid self-assembly in dry conditions. This conclusion is based on combined observations that (i) the dissolution of TMAO is not affected when being present in the lipid systems (Figure 5A), (ii) the position of the $L_{\beta'}$–L_α phase transition in the DMPC system is not altered by TMAO (Figure 5A,B), (iii) the DMPC $L_{\beta'}$ lamellar repeat distance is not affected by the addition of TMAO (Table 1 and Figure S5), and that (iv) at low relative humidities, the measured sorption isotherm for the DMPC $L_{\beta'}$ gel phases with added TMAO overlaps with the theoretical isotherm calculated as a linear combination of the binary DMPC–water and TMAO–water isotherms (Figure 5A, inset). At high water contents, on the other hand, TMAO and urea show a similar effect on the swelling of the L_α lamellar phase (Figure 5C). The experimental data underlying these conclusions will be described in detail below.

In the ternary lipid–TMAO–water systems, the dissolution step of TMAO occurs at 49% RH, which is the same as observed in the binary TMAO–water system (Figures 2C and 5A,C). In the enthalpy curves, this corresponds to endothermic "bumps" at $n_{water}/n_{lipid} \approx 3–6$ (Figures 5B and S3D). The measured ΔH_{sorp} at low water contents is due to a combination of processes, including exothermic heat effects from primary hydration of the PC headgroups and formation of TMAO dihydrates, together with endothermic heat effects from the dissolution of TMAO. These different events at low relative humidities cannot be resolved in the present data and are not analyzed in more detail.

We will first discuss the effect of TMAO on the DMPC self-assembly at varying relative humidities. In the lipid sample with Φ_{TMAO}^{DMPC} = 1 wt %, the $L_{\beta'}$–L_α phase transition is recognized from the sharp increase in the water content (n_{water}/n_{lipid} = 5–12) at 93% RH, which coincides with a region of constant and positive enthalpies (Figure 5B and Table S1). The transition occurs at the same RH as that for the binary DMPC–water system. For the higher TMAO concentration (Φ_{TMAO}^{DMPC} = 10 wt %), the $L_{\beta'}$–L_α phase transition is discerned as a sharp increase in water uptake at 93% RH, corresponding to $n_{water}/n_{lipid} > 20$ (Figure 5A) and in the enthalpy curve at water contents above n_{water}/n_{lipid} = 21 (Figure 5B). In other words, the $L_{\beta'}$–L_α phase transition is not affected by the presence of TMAO. This

DOI: 10.1021/acs.jpcb.8b02159
J. Phys. Chem. B 2018, 122, 6471–6482

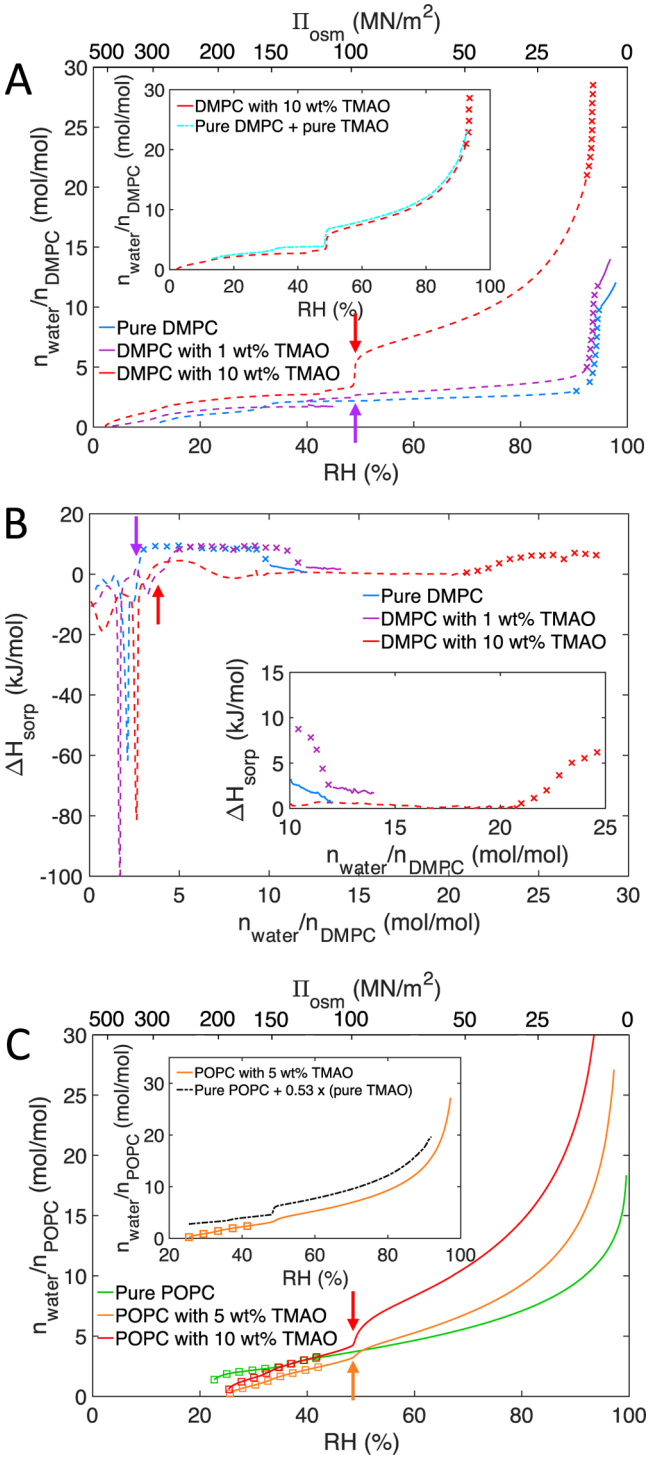

Figure 5. Microcalorimetric sorption data for DMPC and TMAO (A, B), Φ_{TMAO}^{DMPC} = 0, 1 and 10 wt % (blue, purple, and red curves, respectively) and POPC and TMAO (C), Φ_{TMAO}^{POPC} = 0, 5, and 10 wt % (green, orange, and red curves, respectively). (A, C) Sorption isotherms showing water uptake (n_{water}/n_{lipid}) versus relative humidity (% RH) (bottom axis) and the corresponding osmotic pressure of water (Π_{osm}) (top axis). (B) ΔH_{sorp} as a function of water content. The arrows indicate the dissolution step. The phase behavior is represented by: $L_{\beta'}$ gel phase (- -), fluid L_α phase (—), coexistence of $L_{\beta'}$ and L_α phases (xxx), and region where $L_{\beta'}$–L_α transition occurs (exact position not determined) (□□□). Inset in (A) Comparison between the experimental sorption isotherms for sample with composition Φ_{TMAO}^{DMPC} = 10 wt % (red line) and a theoretical ideal isotherm calculated as the linear combination of the experimental isotherms for the binary systems of DMPC–water and TMAO–water with the right proportion to match Φ_{TMAO}^{DMPC} = 10 wt % (cyan line). Inset in (B) shows a magnification of the ΔH_{sorp} at high water content. Inset in (C) comparison between the experimental sorption isotherms for sample with composition Φ_{TMAO}^{POPC} = 5 wt % (orange line) and a theoretical ideal isotherm (black line) calculated as the linear combination of the experimental isotherms for the binary systems of POPC–water and TMAO–water to match Φ_{TMAO}^{POPC} = 5 wt %.

Table 1. Summary of Scattering Data for Lipid Phases with Added TMAO at Different Relative Humidities[a]

lipid	RH (%)	solute	*d* (Å)	phase
DMPC	84	no	54	$L_{\beta'}$
		TMAO 10 wt %	54	$L_{\beta'}$
	96	no	52	L_α
		TMAO 10 wt %	59	L_α
POPC	ca. 1	no	54 and 58	L_{solid}[b]
	43	no	52	L_α
		TMAO 2 wt %	52	L_α
		TMAO 5 wt %	52	L_α
	96	no	53	L_α
		TMAO 2 wt %	57	L_α
		TMAO 5 wt %	59	L_α
		TMAO 10 wt %	59	L_α

[a]Lamellar phase was confirmed for all systems by means of SAXS, which also gives the lamellar repeat distance *d*. WAXS experiments were performed to distinguish between ordered and disordered acyl-chain packing.[56,57] Lipid phase was assigned on the basis of scattering data and previous studies.[32,37,40] TMAO concentration is defined relative to the dry weight of the lipid–TMAO sample Φ_{TMAO}^{lipid}. [b]For the POPC–water system, we did not determine structure of the lamellar phase with ordered chains.

conclusion is also supported by SAXS, WAXS, and PT ssNMR phase characterization for the same systems at selected RH conditions (Table 1, Figures S5, and 4D). The SAXS spectra (Figure S5A) show equidistant Bragg reflections of the lamellar structures both in the presence and the absence of TMAO. At larger diffraction angles (WAXS, Figure S5B), several prominent peaks indicating coexisting ordered solid structures[56,57] are present at 84% RH, whereas no indications of the lamellar gel phase are seen in any of the samples at 96% RH. It is further concluded that the addition of TMAO has no effect on the lamellar repeat distance in the $L_{\beta'}$ phase at 84% RH (Figure S5A). From PT ssNMR experiments, it is also shown that the molecular dynamics of the lipid molecule is not altered by the addition of TMAO at RH = 84% compared to the DMPC–water $L_{\beta'}$ phase at the same relative humidity (Figure 4B,D). Finally, the comparison between the experimental and calculated sorption isotherms at RH < 93% in Figure 5A (inset) indicates that the overall sorption process in the ternary DMPC–TMAO–water system is simply the sum of the processes in the binary systems with no additional interactions. The most likely interpretation of these data is that TMAO is not incorporated in the $L_{\beta'}$ phase. At the lowest relative humidities, TMAO exists as a dry powder and at RH > 43%, TMAO will be dissolved in water to form an aqueous phase that coexists with a lamellar $L_{\beta'}$ phase. The dissolution of TMAO and the dilution of TMAO–water solution lead to substantial water uptake at RH > 49% (Figure 5A). These interpretations are supported by the PT ssNMR data showing

DOI: 10.1021/acs.jpcb.8b02159
J. Phys. Chem. B 2018, 122, 6471–6482

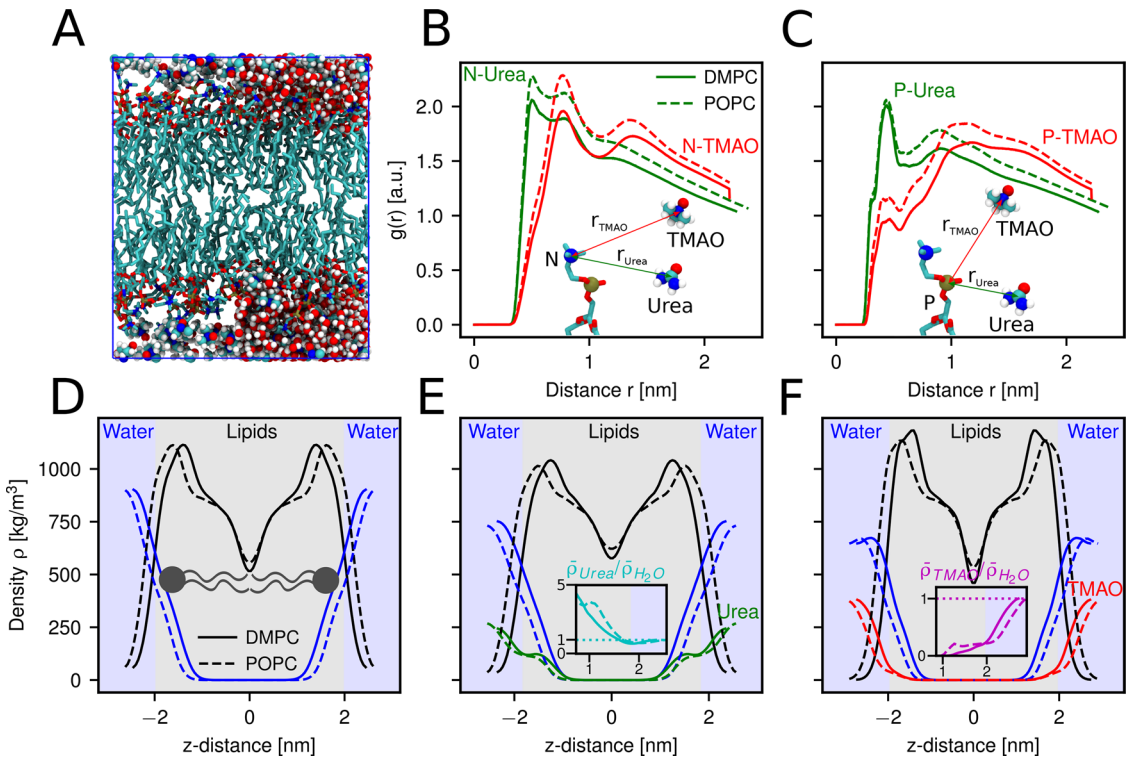

Figure 6. (A) Snapshot of an MD simulation of DMPC at n_{water}/n_{lipid} = 13 with added 10 wt % TMAO (water is only shown on the right half; simulation box is indicated in blue). (B, C) Radial distribution functions $g(r)$ of the lipid headgroup nitrogen (B) and phosphorous (C) atoms for urea (green) and TMAO (red) in lipid systems with 10 wt % solute and n_{water}/n_{lipid} = 13. (D–F) Density profiles of lipids (black), water (blue), urea (green), and TMAO (red) in binary lipid–water systems (D) and lipid–solute–water systems with 10 wt % urea (E) or TMAO (F) at n_{water}/n_{lipid} = 13. Insets show the ratio of solute and water densities, normalized to the respective bulk values. The solid and dashed lines represent DMPC- and POPC-containing systems, respectively.

fast and isotropic reorientation of the TMAO molecule (84% RH, Figure 4D).

When the relative humidity increases above 93%, a single L_α phase is formed in the DMPC–TMAO–water system (Figure 5A,B, Table 1, and Figure S5). In contrast to the low-water-content $L_{\beta'}$ phase, the hydrated L_α phase clearly responds to the addition of TMAO, showing an increased swelling (96% RH in Table 1 and Figure S5A). To investigate the effect of TMAO on the L_α phase over a larger range in hydration conditions, we studied the ternary POPC–TMAO–water systems using the same experimental approach (Φ^{POPC}_{TMAO} = 0, 5, 10 wt %) (Figures 5C and S3D). Again, we confirm that TMAO is dissolved at ca. 49% RH (Figure 5C) and that the lamellar repeat distance is not affected by the addition of TMAO at lower relative humidities (RH < 49%). However, the addition of TMAO causes a rather strong increase in swelling of the L_α phase for RH > 49%. (Figure 5C, Table 1, and Figure S6A,B). It is also shown that the theoretical isotherm calculated as the linear combination of the experimental isotherms for the binary POPC–water and TMAO–water systems for Φ^{POPC}_{TMAO} = 5 wt % clearly deviates from the experimental data at higher relative humidities (inset Figure 5C). This strongly suggests that TMAO is present in the POPC L_α system over a much larger range of RH compared to the DMPC system that forms a gel phase with ordered and rigid chains at RH < 93%. From the analysis of the concentration dependence, it is further concluded that the lipid L_α phase is saturated with TMAO at concentrations around Φ^{POPC}_{TMAO} = 5 wt %, and that excess TMAO is expelled from the lamellar system at higher overall TMAO concentrations. This is inferred from the SAXS data showing that the lamellar repeat distance does not change when increasing the concentration of TMAO above Φ^{POPC}_{TMAO} = 5 wt % (Figure S6B) and from the comparisons between experimental and calculated sorption isotherms at different TMAO concentrations (Figure S7). Finally, we note that the hydration of the L_α phase in the presence of TMAO is associated with small and positive ΔH_{sorp}, as demonstrated for both lipid systems (Figures 5B and S3D).

TMAO is Repelled from the Bilayers Whereas Urea Interacts with the Membrane Interface. The binary lipid–water and ternary lipid–solute–water systems were studied in MD simulations performed in the NpT ensemble at atmospheric pressure and constant temperature (27 °C) for different hydration conditions (illustrated at n_{water}/n_{lipid} = 13 in Figure 6 and n_{water}/n_{lipid} = 25 in Figure S8). The simulations reveal the location of different molecules in terms of density profiles and radial distribution functions (RDFs) of the solutes in relation to the nitrogen and phosphorus of the choline and phosphate of the lipid headgroups. For the binary phospholipid–water system, the water density increases toward the center of the water slab (Figure 6D), approaching the bulk value for neat water at high water contents (shown for n_{water}/n_{lipid} = 25 in Figure S8D). Furthermore, it can be seen that a few water molecules penetrate into the outer parts of the hydrophobic interior of the bilayer, which is also consistent with previous reports.[58,59] The minimum in the DMPC density curve in the middle of the bilayer is known as the 'methyl-dip' and signifies the position where the two monolayers meet in the bilayer center.

DOI: 10.1021/acs.jpcb.8b02159
J. Phys. Chem. B 2018, 122, 6471–6482

A comparison between the profiles in Figure 6E,F clearly demonstrates that urea and TMAO show different affinities to the bilayer interface. In the ternary lipid−solute−water systems, the density profiles and RDFs (Figure 6B,C) show that both urea and TMAO are mainly found in the aqueous slab between the bilayers. However, the systems clearly differ in that urea is accumulated close to the lipid headgroups at the bilayer interface, whereas TMAO is completely repelled from the interfacial layer. The density profile of urea in Figure 6E demonstrates that some urea molecules penetrate into the outer part of the hydrophobic region of the bilayer where the urea/water ratio is significantly higher compared to that in the aqueous slab (inset in Figure 6E). The RDFs for urea further show distinct peaks near the POPC and DMPC headgroups (Figure 6B,C). The TMAO-density profile, on the other hand, declines rapidly when approaching the headgroup layer from the aqueous slab, and the same result is apparent in the corresponding RDFs (Figure 6F and B,C). The density profiles further suggest that the TMAO/water ratio in the outer layer of the bilayer is much lower compared with the concentration in the water slab (inset in Figure 6F). The RDFs in Figure 6B,C also show that TMAO is more repelled from the positively charged choline group compared with urea and a similar and more long-ranged effect is also observed for the negatively charged phosphate group of the lipid headgroup. As DMPC and POPC differ only in the composition of their hydrocarbon tails, it is not surprising that the solute-headgroup interactions do not significantly differ between these systems.

DISCUSSION

Osmolytes are small polar molecules with low vapor pressure that are commonly used in nature to protect biomolecular systems against osmotic stress and to prevent dehydration-induced structural changes in macromolecular assemblies. Here, we confirm that urea has the ability to protect lipid membranes against osmotic stress by preventing dehydration-induced lipid phase transitions (Figures 3 and 4, Table S1), which is consistent with previous studies.[31,32] Similar behavior has also been reported for other small polar solutes, including glycerol[31] and sugars.[33,34] It is notable that even though urea and other polar solutes will mainly be found in the aqueous layers of the lipid lamellar phases, they still show strong effects on the solid−fluid transition in the hydrophobic chains of the lipid bilayers. These polar solutes may exchange for water in the lipid lamellar systems in such a way that the properties of the lipid bilayer remain largely unaffected, and for lipid systems with limited access to solvent, the phase behavior is determined by the solvent volume irrespective of the composition.[32] With this perspective, it may seem surprising that when urea is exchanged with another small polar molecule, TMAO (Figure 5 and Table S1), the protection against dehydration-induced changes in lipid self-assembly is not observed.

We here demonstrate that urea and TMAO have clearly different effects on dehydration-induced lipid phase transitions. In the more hydrated system, on the other hand, TMAO and urea influence lipid self-assembly in qualitatively similar ways (Figures 3 and 5). These findings can be explained by the differences in the molecular interactions between the solutes and the lipid headgroups. In MD simulations (Figure 6B−F), it was shown that TMAO is depleted from the region close to the bilayer interface, whereas urea shows a slight affinity to the lipid headgroup region. For the case of TMAO, the total thickness of the depletion layers in between the bilayers in the lamellar phase is estimated to be ca. 2 nm (Figure 6F), which is similar to the total thickness of the aqueous region between the DMPC $L_{\beta'}$ phase bilayers at 84% RH (Table 1). The thickness of the aqueous region including the headgroups was calculated assuming a bilayer thickness of 30 Å.[60] In other words, the TMAO molecules will likely be expelled from the lamellar phase for all lamellar systems with narrow inter-bilayer separations. For these conditions, TMAO will instead be found in a segregated TMAO−water phase with the same water chemical potential as that of the lipid lamellar phase, which, for the present set-up, is determined by the RH in the vapor phase (eq 1). As TMAO is not present in the lamellar $L_{\beta'}$ gel phase, it cannot substitute for water upon drying and it will not affect the lipid self-assembly at low water contents. However, when the thickness of the inter-bilayer water region is larger than the thickness of the depletion layers close to the lipid headgroups, TMAO can partition into the water regions in the lamellar system and it may then act in a similar way as other polar solutes with low vapor pressure. This is illustrated here for urea and TMAO in the L_α phase at high water content (Figures 3A,C and 5C). One way to test this proposed mechanism of how TMAO influences lipid lamellar systems at varying water contents is to increase the water separation in the solid phase by adding a small amount of charged lipids. By supplementing the DMPC bilayer system with 5 mol % anionic dimyristoyl phosphoglycerol (DMPG), the lamellar repeat distance in the solid phase will increase due to the electrostatic repulsion (Table S3), thereby increasing TMAO partitioning into lamellar phase. Indeed, for the DMPC−DMPG system, both urea and TMAO were shown to stabilize the L_α phase over the $L_{\beta'}$ phase (Table S3). The emerging picture from the combination of data in Figures 3−6 and Table 1, S1 is a mechanism where the interactions between lipids and solutes are crucial for dry systems with high concentrations of lipid and solute. The role of the specific solute−lipid interactions will become less significant when the water content of the system increases. When the lamellar phase is sufficiently swollen, the molecular nature of the polar solute becomes less important and the unspecific mechanism of water replacement applies.

From the combined experimental data in Table 1 and Figures 5 and S5−S7, we conclude that TMAO is expelled from the lipid lamellar systems to form a segregated phase for all conditions where the total concentration of TMAO exceeds the saturation limit in the lipid lamellar phase. The saturation limit in the lamellar phase will depend on the distribution profiles of TMAO and water in the inter-bilayer regions at the given water chemical potential, as determined by the relative humidity of the vapor phase. Segregation will thus occur at low relative humidities, as discussed above, as well as at high overall TMAO concentrations. For the model system of POPC, we conclude that the addition of TMAO at a concentration above the estimated saturation concentration of 5 wt % TMAO relative to the lipid has no effect on the lipid self-assembly (Figures S6B and S7). The conditions investigated here correspond to samples that are in contact with a vapor phase and differ from conditions where the lipid lamellar phase is dispersed in an excess solution with a given concentration of TMAO. In the latter case, the chemical potential of water, and thus the osmotic pressure, will be determined by the concentration of solute in the excess aqueous solution. If the concentration of TMAO is increased above its saturation limit in the lamellar system, the excess amount of TMAO will be depleted from the lamellar system, causing an increased osmotic pressure and an

DOI: 10.1021/acs.jpcb.8b02159
J. Phys. Chem. B 2018, 122, 6471−6482

imbalance in TMAO distribution between the bulk and the inter-bilayer space in the lamellar phase, thereby leading to reduced inter-bilayer separation in the lamellar phase. This situation was recently analyzed in combined experimental and theoretical studies by Sukenik et al.[36]

The observed differences at low hydration conditions can be explained by differences in the molecular interactions between the solutes and the lipid headgroups. Urea features a dipole and is therefore able to interact favorably with the PC motif, in particular, with the negatively charged phosphate group (Figure 6). As a result, urea is not excluded from the interlamellar water layers. TMAO, on the other hand, possesses a strong electrical dipole of which the positive charge is capped with hydrophobic methyl groups. The phosphatidylcholine (PC) headgroup of DMPC and POPC exhibits the same dipolar/hydrophobic architecture. It has been shown that dipolar/hydrophobic motifs experience mutual repulsion in aqueous environments,[27] which explains why TMAO is excluded from the membrane surfaces and thus from the interlamellar water layers as long as they are thin enough. It is noted here that it was previously suggested that TMAO locates close to the PC headgroups and exhibits a specific orientation effect in the headgroup layer on the basis of vibrational sum frequency generation spectroscopy studies of liquid condensed dipalmitoylphosphatidylcholine monolayers.[61] This conclusion is not consistent with the simulation data in Figure 6, although direct comparisons cannot be drawn as the condensed monolayer and liquid crystalline lamellar systems widely differ.

There are several examples of biological systems where TMAO and urea are both present at relatively high concentrations.[10,17,18] Urea and TMAO show opposite effects on protein stability, where urea is known to act as a protein denaturant, whereas TMAO can stabilize folded protein structures.[27−29] When it comes to interactions with phospholipid membranes, both urea and TMAO may substitute water in an unspecific way and thereby prevent dehydration-induced phase transitions, which has also been shown for other uncharged osmolytes.[31,33,34] These polar compounds can therefore be described as stabilizers in membrane systems under osmotic stress. However, the ability of the different polar compounds to stabilize lipid membranes in dry conditions is strongly dependent on the specific interactions between the solute and the lipid bilayer. As TMAO is repelled from the bilayer interface and thereby excluded from lamellar systems at dry conditions, it is inferred that TMAO is not efficient in protecting phospholipid membranes from dehydration-induced phase changes in very dry conditions. It is possible that the combined effect of TMAO and urea is to both protect membranes against severe dehydration and still avoid denaturation of proteins.

■ ASSOCIATED CONTENT

Supporting Information

The Supporting Information is available free of charge on the ACS Publications website at DOI: 10.1021/acs.jpcb.8b02159.

Phase transition regime in the DMPC−solute−water systems (Table S1); dissolution RH of solutes in different systems (Table S2); summary of scattering data for DMPC−DMPG lipid systems with added solute (Table S3); osmotic pressure for DMPC and POPC (Figure S1); scattering data of POPC−water and POPC−TMAO−water systems (Figure S2); sorption enthalpy of water for urea, TMAO, POPC and urea, and POPC and TMAO systems (Figure S3); sorption isotherms of L_α phase of lipid−urea−water systems (Figure S4); scattering data of DMPC−TMAO−water systems (Figure S5); SAXS data of POPC−TMAO−water systems (Figure S6); comparison between the experimental sorption isotherms for POPC−TMAO−water system and a theoretical ideal isotherm (Figure S7); MD simulation at n_{water}/n_{lipid} = 25 (Figure S8) (PDF)

■ AUTHOR INFORMATION

Corresponding Author

*E-mail: dat.pham@fkem1.lu.se.

ORCID

Quoc Dat Pham: 0000-0003-3267-8580

Emanuel Schneck: 0000-0001-9769-2194

Notes

The authors declare no competing financial interest.

■ ACKNOWLEDGMENTS

The Swedish Research Council (VR) is gratefully acknowledged for financial support both through regular grants and the Linnaeus Center of Excellence "Organizing molecular matter" (E.Sparr). The Swedish Foundation for Strategic Research Strategic Research (E.Sparr), the Crafoord Foundation Strategic Research (E.Sparr), and the Royal Physiographic Society of Lund (Q.D.P.) are acknowledged for financial support. R.R.N. and A.W.-K. acknowledge support by the DFG via grant 1112. E.Schneck acknowledges support by the Max Planck Society and by the German Research Foundation (DFG) via Emmy-Noether grant (SCHN 1396/1). We thank Lars Wadsö and Vitaly Kocherbitov for help with the sorption calorimetry measurements and analysis. We kindly acknowledge Håkan Wennerström for fruitful discussions.

■ ADDITIONAL NOTE

[a]For the DMPC−water system, the planar gel phase has been assigned to $L_{\beta'}$ with tilted acyl chains. Here, we use the same terminology without further investigation of how hydration and addition of solutes influence the chain tilting in the planar gel phase.

■ REFERENCES

(1) Janiak, M. J.; Small, D. M.; Shipley, G. G. Temperature and Compositional Dependence of the Structure of Hydrated Dimyristoyl Lecithin. *J. Biol. Chem.* **1979**, *254*, 6068−6078.

(2) Xiang, T.-X.; Anderson, B. D. Phase Structures of Binary Lipid Bilayers as Revealed by Permeability of Small Molecules. *Biochim. Biophys. Acta, Biomembr.* **1998**, *1370*, 64−76.

(3) Steponkus, P. L. Freeze-Induced Dehydration and the Cryostability of Biological Membranes. In *Water Management in Design and Distribution of Quality Foods*; Poos, Y. H.; Leslie, R. B.; Lillford, P. J., Eds.; Technomic Publishing Co. Inc., Lancaster: Basel, 1999; pp 53−85.

(4) Björklund, S.; Engblom, J.; Thuresson, K.; Sparr, E. A Water Gradient Can Be Used to Regulate Drug Transport across Skin. *J. Controlled Release* **2010**, *143*, 191−200.

(5) Blank, I. H.; Moloney, J., III.; Emslie, A. G.; Simon, I.; Apt, C. The Diffusion of Water across the Stratum Corneum as a Function of its Water Content. *J. Invest. Dermatol.* **1984**, *82*, 188−194.

(6) Zhai, H.; Maibach, I. Occlusion vs Skin Barrier Function. *Skin Res. Technol.* **2002**, *8*, 1−6.

DOI: 10.1021/acs.jpcb.8b02159
J. Phys. Chem. B 2018, 122, 6471−6482

(7) Björklund, S.; Nowacka, A.; Bouwstra, J. A.; Sparr, E.; Topgaard, D. Characterization of Stratum Corneum Molecular Dynamics by Natural-Abundance 13C Solid-State NMR. *PLoS One* **2013**, *8*, No. e61889.
(8) Rand, R. P. Probing the Role of Water in Protein Conformation and Function. *Philos. Trans. R. Soc., B* **2004**, *359*, 1277−1285.
(9) Mansouri, A. L.; Grese, L. N.; Rowe, E. L.; Pino, J. C.; Chennubhotla, S. C.; Ramanathan, A.; O'Neill, H. M.; Berthelier, V.; Stanley, C. B. Folding Propensity of Intrinsically Disordered Proteins by Osmotic Stress. *Mol. Biosyst.* **2016**, *12*, 3695−3701.
(10) Storey, K. B.; Storey, J. M. Freeze Tolerance in Animals. *Physiol. Rev.* **1988**, *68*, 27−84.
(11) Yancey, P. H. Organic Osmolytes as Compatible, Metabolic, and Counteracting Cytoprotectants in High Osmolarity and Other Stresses. *J. Exp. Biol.* **2005**, *208*, 2819−2830.
(12) Harries, D.; Rösgen, J. A Practical Guide on How Osmolytes Modulate Macromolecular Properties. *Methods Cell Biol.* **2008**, *84*, 679−735.
(13) Vereyken, I. J.; Chupin, V.; Islamov, A.; Kuklin, A.; Hincha, D. K.; de Kruijff, B. The Effect of Fructan on the Phospholipid Organization in the Dry State. *Biophys. J.* **2003**, *85*, 3058−3065.
(14) Crowe, J. H.; Hoekstra, F. A.; Crowe, L. M. Anhydrobiosis. *Annu. Rev. Physiol.* **1992**, *54*, 579−599.
(15) Kirst, G. O. Salinity Tolerance of Eukaryotic Marine-Algae. *Annu. Rev. Plant Physiol. Plant Mol. Biol.* **1990**, *41*, 21−53.
(16) Ramloy, U.-B. Aspects of Natural Cold Tolerance in Ectothermic Animals. *Hum. Reprod.* **2000**, *15*, 26−46.
(17) Perlman, D. F.; Goldstein, L. Nitrogen Metabolism. In *Physiology of Elasmobranch Fishes*; Shuttleworth, T. J., Ed.; Springer-Verlag: New York, 1989; pp 253−273.
(18) Barton, K. N.; Buhr, M. M.; Ballantyne, J. S. Effects of Urea and Trimethylamine N-Oxide on Fluidity of Liposomes and Membranes of an Elasmobranch. *Am. J. Physiol.: Regul., Integr. Comp. Physiol.* **1999**, *276*, R397−R406.
(19) Hara, M.; Verkman, A. S. Glycerol Replacement Corrects Defective Skin Hydration, Elasticity, and Barrier Function in Aquaporin-3-Deficient Mice. *Proc. Natl. Acad. Sci. U.S.A.* **2003**, *100*, 7360−7365.
(20) Choi, E. H.; Man, M. Q.; Wang, F. S.; Zhang, X. J.; Brown, B. E.; Feingold, K. R.; Elias, P. M. Is Endogenous Glycerol a Determinant of Stratum Corneum Hydration in Humans? *J. Invest. Dermatol.* **2005**, *125*, 288−293.
(21) Rawlings, A. V.; Scott, I. R.; Harding, C. R.; Bowser, P. A. Stratum Corneum Moisturization at the Molecular Level. *J. Invest. Dermatol.* **1994**, *103*, 731−740.
(22) Björklund, S.; Andersson, J. M.; Pham, Q. D.; Nowacka, A.; Topgaard, D.; Sparr, E. Stratum Corneum Molecular Mobility in the Presence of Natural Moisturizers. *Soft Matter* **2014**, *10*, 4535−4546.
(23) Katagiri, C.; Sato, J.; Nomura, J.; Denda, M. Changes in Environmental Humidity Affect the Water-Holding Property of the Stratum Corneum and its Free Amino Acid Content, and the Expression of Filaggrin in the Epidermis of Hairless Mice. *J. Dermatol. Sci.* **2003**, *31*, 29−35.
(24) Kezic, S.; O'Regan, G. M.; Yau, N.; Sandilands, A.; Chen, H.; Campbell, L. E.; Kroboth, K.; Watson, R.; Rowland, M.; McLean, W. H.; et al. Levels of Filaggrin Degradation Products Are Influenced by Both Filaggrin Genotype and Atopic Dermatitis Severity. *Allergy* **2011**, *66*, 934−940.
(25) Mehnert, W.; Mader, K. Solid Lipid Nanoparticles Production, Characterization and Applications. *Adv. Drug Delivery Rev.* **2012**, *64*, 83−101.
(26) Lodén, M. Role of Topical Emollients and Moisturizers in the Treatment of Dry Skin Barrier Disorders. *Am. J. Clin. Dermatol.* **2003**, *4*, 771−788.
(27) Schneck, E.; Horinek, D.; Netz, R. R. Insight into the Molecular Mechanisms of Protein Stabilizing Osmolytes from Global Force-Field Variations. *J. Phys. Chem. B* **2013**, *117*, 8310−8321.
(28) Lin, T.-Y.; Timasheff, S. N. Why Do Some Organisms Use a Urea-Methylamine Mixture as Osmolyte? Thermodynamic Compensation of Urea and Trimethylamine N-Oxide Interactions with Protein. *Biochemistry* **1994**, *33*, 12695−12701.
(29) Ma, J.; Pazos, I. M.; Gai, F. Microscopic Insights into the Protein-Stabilizing Effect of Trimethylamine N-Oxide (TMAO). *Proc. Natl. Acad. Sci. U.S.A.* **2014**, *111*, 8476−8481.
(30) Yancey, P. H.; Somero, G. N. Counteraction of Urea Destabilization of Protein Structure by Methylamine Osmoregulatory Compounds of Elasmobranch Fishes. *Biochem. J.* **1979**, *183*, 317−323.
(31) Nowacka, A.; Douezan, S.; Wadso, L.; Topgaard, D.; Sparr, E. Small Polar Molecules like Glycerol and Urea Can Preserve the Fluidity of Lipid Bilayers under Dry Conditions. *Soft Matter* **2012**, *8*, 1482−1491.
(32) Costa-Balogh, F. O.; Wennerström, H.; Wadsö, L.; Sparr, E. How Small Polar Molecules Protect Membrane Systems against Osmotic Stress: The Urea-Water-Phospholipid System. *J. Phys. Chem. B* **2006**, *110*, 23845−23852.
(33) Crowe, J. H.; Crowe, L. M.; Chapman, D. Preservation of Membranes in Anhydrobiotic Organisms: the Role of Trehalose. *Science* **1984**, *223*, 701−703.
(34) Crowe, L. M.; Crowe, J. H. Solution Effects on the Thermotropic Phase Transition of Unilamellar Liposomes. *Biochim. Biophys. Acta, Biomembr.* **1991**, *1064*, 267−274.
(35) McDaniel, R. V.; McIntosh, T. J.; Simon, S. A. Nonelectrolyte Substitution for Water in Phosphatidylcholine Bilayers. *Biochim. Biophys. Acta, Biomembr.* **1983**, *731*, 97−108.
(36) Sukenik, S.; Dunsky, S.; Barnoy, A.; Shumilin, I.; Harries, D. TMAO Mediates Effective Attraction between Lipid Membranes by Partitioning Unevenly between Bulk and Lipid Domains. *Phys. Chem. Chem. Phys.* **2017**, *19*, 29862−29871.
(37) Binder, H.; Klose, G. Lyotropic Phase Behavior and Structure of Mixed Lipid (POPC)-Detergent (C12En, n = 2, 4, 6) Assemblies: Insights from Hydration-Tuning Infrared Spectroscopy. *J. Phys. Chem. B* **2002**, *106*, 10991−11001.
(38) Nilsson, A.; Holmgren, A.; Lindblom, G. Fourier-Transform Infrared-Spectroscopy Study of Dioleoylphosphatidylcholine and Monooleoylglycerol in Lamellar and Cubic Liquid-Crystals. *Biochemistry* **1991**, *30*, 2126−2133.
(39) Mcintosh, T. J.; Magid, A. D.; Simon, S. A. Steric Repulsion between Phosphatidylcholine Bilayers. *Biochemistry* **1987**, *26*, 7325−7332.
(40) Markova, N.; Sparr, E.; Wadsö, L.; Wennerström, H. A Calorimetric Study of Phospholipid Hydration. Simultaneous Monitoring of Enthalpy and Free Energy. *J. Phys. Chem. B* **2000**, *104*, 8053−8060.
(41) Wadsö, L.; Markova, N. A Method to Simultaneously Determine Sorption Isotherms and Sorption Enthalpies with a Double Twin Microcalorimeter. *Rev. Sci. Instrum.* **2002**, *73*, 2743−2754.
(42) Pines, A.; Gibby, M. G.; Waugh, J. S. Proton-Enhanced Nuclear Induction Spectroscopy. A Method for High Resolution NMR of Dilute Spins in Solids. *J. Chem. Phys.* **1972**, *56*, 1776−1777.
(43) Morris, G. A.; Freeman, R. Enhancement of Nuclear Magnetic-Resonance Signals by Polarization Transfer. *J. Am. Chem. Soc.* **1979**, *101*, 760−762.
(44) Vangeet, A. L. Calibration of Methanol Nuclear Magnetic Resonance Thermometer at Low Temperature. *Anal. Chem.* **1970**, *42*, 679−680.
(45) Bennett, A. E.; Rienstra, C. M.; Auger, M.; Lakshmi, K. V.; Griffin, R. G. Heteronuclear Decoupling in Rotating Solids. *J. Chem. Phys.* **1995**, *103*, 6951−6958.
(46) van Beek, J. D. matNMR: A Flexible Toolbox for Processing, Analyzing and Visualizing Magnetic Resonance Data in Matlab. *J. Magn. Reson.* **2007**, *187*, 19−26.
(47) Nowacka, A.; Bongartz, N. A.; Ollila, O. H.; Nylander, T.; Topgaard, D. Signal Intensities in 1H-13C CP and INEPT MAS NMR of Liquid Crystals. *J. Magn. Reson.* **2013**, *230*, 165−175.
(48) Tieleman, D. P.; Forrest, L. R.; Sansom, M. S.; Berendsen, H. J. Lipid Properties and the Orientation of Aromatic Residues in OmpF, Influenza M2, and Alamethicin Systems: Molecular Dynamics Simulations. *Biochemistry* **1998**, *37*, 17554−17561.

DOI: 10.1021/acs.jpcb.8b02159
J. Phys. Chem. B 2018, 122, 6471−6482

(49) Berger, O.; Edholm, O.; Jähnig, F. Molecular Dynamics Simulations of a Fluid Bilayer of Dipalmitoylphosphatidylcholine at Full Hydration, Constant Pressure, and Constant Temperature. *Biophys. J.* **1997**, *72*, 2002−2013.
(50) Berendsen, H. J. C.; Grigera, J. R.; Straatsma, T. P. The Missing Term in Effective Pair Potentials. *J. Phys. Chem.* **1987**, *91*, 6269−6271.
(51) Horinek, D.; Netz, R. R. Can Simulations Quantitatively Predict Peptide Transfer Free Energies to Urea Solutions? Thermodynamic Concepts and Force Field Limitations. *J. Phys. Chem. A* **2011**, *115*, 6125−6136.
(52) Bussi, G.; Donadio, D.; Parrinello, M. Canonical Sampling through Velocity Rescaling. *J. Chem. Phys.* **2007**, *126*, No. 014101.
(53) Berendsen, H. J. C.; Postma, J. P. M.; van Gunsteren, W. F.; DiNola, A.; Haak, J. R. Molecular Dynamics with Coupling to an External Bath. *J. Chem. Phys.* **1984**, *81*, 3684−3690.
(54) Pohle, W.; Selle, C.; Fritzsche, H.; Binder, H. Fourier Transform Infrared Spectroscopy as a Probe for the Study of the Hydration of Lipid Self-Assemblies. I. Methodology and General Phenomena. *Biospectroscopy* **1998**, *4*, 267−280.
(55) Mak, T. C. W. Crystal-Structure of Trimethylamine Oxide Dihydrate. *J. Mol. Struct.* **1988**, *178*, 169−175.
(56) Tardieu, A.; Luzzati, V.; Reman, F. C. Structure and Polymorphism of the Hydrocarbon Chains of Lipids: A Study of Lecithin-Water Phases. *J. Mol. Biol.* **1973**, *75*, 711−733.
(57) Tenchov, B.; Koynova, R.; Rapp, G. New Ordered Metastable Phases between the Gel and Subgel Phases in Hydrated Phospholipids. *Biophys. J.* **2001**, *80*, 1873−1890.
(58) Wiener, M. C.; White, S. H. Structure of a Fluid Dioleoylphosphatidylcholine Bilayer Determined by Joint Refinement of X-Ray and Neutron Diffraction Data. III. Complete Structure. *Biophys. J.* **1992**, *61*, 434−447.
(59) Marrink, S. J.; Berendsen, H. J. C. Simulation of Water Transport through a Lipid Membrane. *J. Phys. Chem.* **1994**, *98*, 4155−4168.
(60) Tristram-Nagle, S.; Liu, Y. F.; Legleiter, J.; Nagle, J. F. Structure of Gel Phase DMPC Determined by X-ray Diffraction. *Biophys. J.* **2002**, *83*, 3324−3335.
(61) Mondal, J. A. Effect of Trimethylamine N-Oxide on Interfacial Electrostatics at Phospholipid Monolayer−Water Interfaces and its Relevance to Cardiovascular Disease. *J. Phys. Chem. Lett.* **2016**, *7*, 1704−1708.

DOI: 10.1021/acs.jpcb.8b02159
J. Phys. Chem. B 2018, 122, 6471−6482